

# CALIBRATION OF HIGH FIDELITY BARE ROD BUNDLE SIMULATIONS FOR VARIOUS PRANDTL FLUIDS

**T. Cardoso de Souza, A. Shams, F. Roelofs**

Nuclear Research and Consultancy Group (NRG)  
Westerduinweg 3, PO Box 25, 1755 ZG Petten, The Netherlands  
[cardoso@nrg.eu](mailto:cardoso@nrg.eu), [shams@nrg.eu](mailto:shams@nrg.eu), [roelofs@nrg.eu](mailto:roelofs@nrg.eu)

**T. Kwiatkowski**

National Center for Nuclear Research  
ul. Andrzeja Sołtana 7, 05-400 Otwock-Świerk, Poland  
[tomasz.kwiatkowski@ncbj.gov.pl](mailto:tomasz.kwiatkowski@ncbj.gov.pl)

## ABSTRACT

One of the key factors in the design of liquid metal cooled fast reactors (LMFRs) refers to the detailed knowledge of the coolant flow in the sub-channels of the fuel assemblies in the reactor's core. In fact, a thorough experimental investigation of the flow mixing and heat transport in such sub-channels is often impossible or quite costly to be performed. Due to these limitations, computational fluid dynamics (CFD) has recently become a valuable tool in the study of the dynamics of the flow within the sub-channel regions of typical nuclear fuel assemblies.

In general, RANS (Reynolds Averaged Navier-Stokes) approaches are used to analyze the flow and mixing processes within fuel assemblies. In some cases LES (Large eddy simulation) could also be used. Nevertheless, both RANS and LES modeling are associated with numerical errors derived from the averaged/filtered Navier-Stokes equations, which in turn impose significant limitations especially in the modeling of low Prandtl fluids, used as coolant in LMFRs. In addition, the lack of experimental database or additional reference data, e.g. fully detailed high fidelity DNS, often limits the reliability of traditional RANS and LES approaches in modeling flow and heat transfer in liquid metal cooled reactors.

In this paper, through a calibration procedure of the mass flow rate of a sub-channel geometry characteristic of LMFRs fuel assemblies, an approach is developed to obtain the required resolution for a computationally affordable high fidelity DNS of sub-channel flow. As a first step, the sub-channel geometry of a well-documented case is adopted; the hydraulic experiments performed by Hooper on a tight lattice bare rod-bundle configuration which uses air as the working fluid. Subsequently, a set of URANS simulations are performed in which the experimental mass flow rate was systematically scaled in order to estimate a feasible resolution to perform a high fidelity DNS of Hooper's sub-channel flow. Finally, on a sub-channel configuration with  $P/D=1.32$ , a set of URANS simulations for different working fluids (air, water, and liquid lead) are additionally performed. Despite the large variability of the fluid properties, results show that the overall flow physics typical of sub-channels, e.g. large-scale macroscopic pulsations, is identical in all cases provided the bulk Reynolds number is the same. In general, these results show that the detailed DNS data to be obtained for Hooper's case will provide a valuable resource reference for turbulence modeling validation of liquid metal sub-channel flows in LMFRs fuel bundles.

## KEYWORDS

LMFR, URANS, DNS, Hooper, bare rod bundle

## 1. INTRODUCTION

Liquid metal cooled fast reactors (LMFRs) are considered as a promising alternative for future nuclear energy technologies. One of the key advantages for the deployment of such reactors refers to the possibility of reducing the volume and lifetime of the nuclear waste in combination with its efficient use of the nuclear fuel [1, 2, 3].

The nuclear chain reaction, which is the source of nuclear fission energy production, takes place in the core of a nuclear reactor. Within this core, heat is produced in nuclear fuel and transported to a coolant. Mostly, nuclear cores consist of a few hundred fuel assemblies which in turn consist of a large number of fuel rods. In the specific case of LMFRs, single phase heat transfer plays therefore an important role in the thermal-hydraulic evaluation of the reactor core. Historically, such metal cooled reactors employ wire wraps as spacers in the fuel assemblies [1]. However, some designs aim at employing grid spacers. One such an example is the Advanced Lead Fast Reactor European Demonstrator (ALFRED) [4, 5], which aims at employing grid spacers. When employing grid spacers, the axial coolant flow in the fuel pin assembly could cause vibrations resulting from fluid-structure interactions. The knowledge and understanding of these vibrations is critical to estimate the lifetime of the fuel pin with regard to structural integrity and mechanical wear, such as fretting. Knowledge of the expected vibrations will also provide input on the required manufacturing tolerances of the fuel assembly. In reactors employing grid spacers, the axial distance between grid spacers is relatively large compared to the pitch of the individual rods. Therefore, the flow which is disturbed because of the presence of grid spacers, will redevelop in axial direction. Such a flow can be well represented by a bare rod bundle, i.e. a rod bundle not employing any spacers at all.

In general the detailed design and safety analysis of LMFR fuel assemblies is often limited by a lack of experimental data. In fact, experimental measurements of the flow mixing and heat transport in the sub-channels of a fuel assembly is frequently impossible or quite costly to be performed. And even when experimental data is available, the restrictions of performing measurements in the small space available lead to limitations in the available data. To overcome this knowledge gap, computational fluid dynamics (CFD) has recently become a valuable research tool to analyze the complex fuel assembly thermal hydraulics of LMFRs.

As mentioned, a detailed knowledge of the flow mixing and heat transport in these regions is essential for design and safety analysis of LMFRs, since localized flow effects, e.g., hot spots, thermo-mechanical loads, partial blockage effects and deformation [3], which are often related with the flow of the coolant fluid within these sub-channels, for instance, are not accounted in traditionally applied design systems codes, e.g., RELAP [3]. In such cases, common CFD approaches, e.g., RANS (Reynolds Averaged Navier-Stokes) are often used to analyze the flow and turbulent mixing processes within these fuel assemblies [3]. Since an accurate simulation of heat transport is frequently required, for some cases LES (Large eddy simulation) can also be used. Nevertheless, RANS (and to some respect even LES) modeling approaches are inherently associated with numerical errors derived from the averaged Navier-Stokes equations, which in turn impose significant limitations especially in the modeling of low Prandtl fluids, as the case of LMFRs [3]. The lack of experimental database or additional reference data, e.g. fully detailed high fidelity DNS (Direct Numerical Simulation), limits the reliability of traditional CFD approaches in modeling flow and heat transfer in LMFRs.

Although DNS would be preferable, since the modeling errors are kept to a minimum while the only effective error source derives from the numerical discretization, its application is frequently limited by the high computational costs associated with the required spatial resolution, which is especially critical for flows at high Reynolds number as in LMFRs. This limitation often restricts the applicability of this methodology to relatively simple flow geometries. Despite these difficulties, in this paper, through a calibration procedure of the mass flow rate in a sub-channel geometry characteristic of LMFRs fuel assemblies, we develop an approach to obtain the required resolution for a computationally affordable high fidelity DNS of a sub-channel flow. This paper forms the basis of a further numerical investigation where a detailed reference simulation of the coolant fluid flow through a sub-channel configuration typical of LMFRs will be pursued.

To establish our approach, firstly we select a sub-channel geometry of a well-documented case; the hydraulic experiments performed by Hooper on a tight lattice bare rod-bundle configuration (with pitch-to-diameter ratio  $P/D=1.107$ ) which uses air as the working fluid [6]. As a second step, a set of unsteady RANS simulations were performed in which the experimental mass flow rate was systematically scaled, while keeping the same Reynolds number of the experiments, in order to estimate a computationally affordable spatial resolution of a high fidelity simulation of Hooper's sub-channel flow.

Finally, on a sub-channel configuration with pitch-to-diameter ratio of  $P/D=1.32$ , a set of unsteady RANS simulations for different working fluids, e.g., air, water, and liquid lead, were performed. We want to analyze whether despite the large variability of the fluid properties, the sub-channel flow physics show similarities.

The structure of this paper is as follows. In section 2, the layout of the computational model, including the sub-channel of Hooper's geometry, is outlined. The mass flow calibration procedure will also be introduced in this section. In section 3, the results of the sub-channel flow for Hooper's bare rod bundle configuration are assessed, together with a detailed description of the systematic scaling of the mass flow rate and an estimation of the mesh size for the high fidelity DNS to be performed. Subsequently, in section 4, results of a sub-channel configuration with pitch-to-diameter ratio of  $P/D=1.32$  will be discussed for several types of coolant fluids. Concluding remarks are contained in section 5.

## 2. LAYOUT OF COMPUTATIONAL MODEL

In this section, a detailed description of the sub-channel geometry associated with Hooper's bare rod bundle configuration is given [6]. Further details on the CFD numerical modeling, e.g., boundary conditions, turbulence model, and the main flow parameters, i.e., bulk Reynolds number, experimental mass flow rate, are also addressed.

As already mentioned, this paper focuses on the numerical analysis of sub-channel flows on bare rod bundles, i.e., fuel rods without spacers [3]. The adopted reference case is based on the sub-channel geometry of Hooper's hydraulic experiments [6]. This configuration consists on a squared pitched tight lattice bare rod-bundle of pitch-to-diameter ratio of  $P/D=1.107$ . Figure 1 shows the geometry and the selected numerical domain of Hooper's sub-channel.

In Hooper's experiments, the working fluid is air at room temperature conditions and atmospheric pressure. At the inlet, as in the experiments, an uniform air mass flow rate of  $\dot{m}_e = 0.052 \text{ kg/s}$  was initially imposed. Based on the sub-channel hydraulic diameter this leads to a bulk Reynolds number of  $Re_{bulk} \approx 49000$ .

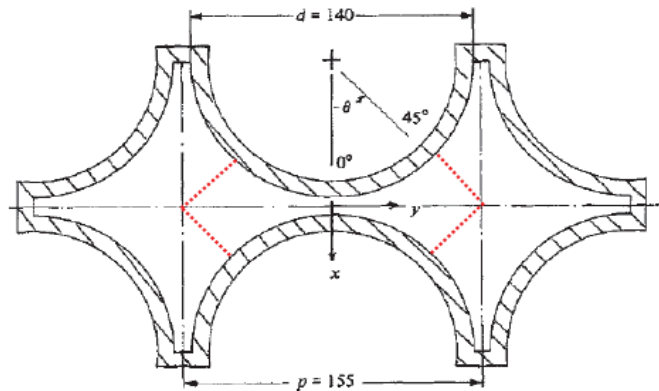


**Figure 1. Sub-channel cross section of Hooper's hydraulic experiment. The red dotted line represents the selected region for the sub-channel CFD numerical analysis.**

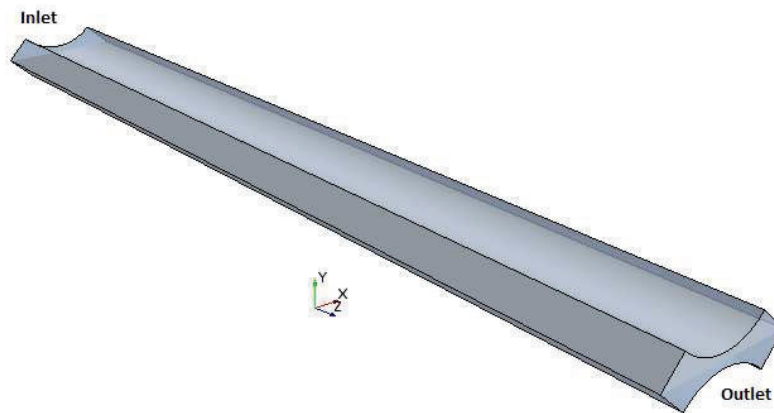


**Figure 2. Numerical domain of Hooper's sub-channel. The inlet and outlet regions are shown with the dashed arrows indicating the main direction of the flow. On the sloped lateral sides symmetric boundaries are applied.**

In this paper, the system of Navier-Stokes equations is solved using an incompressible formulation with OpenFOAM v2.2.0 [10] as the CFD code. Momentum equations are integrated in time using the second order implicit backward method. For all cases, a large-time step transient solver for incompressible flows is applied, e.g. pimpleFoam [10], with pressure-velocity coupling treated using the PIMPLE algorithm [10]. To model the flow within Hooper's sub-channel configuration, a series of numerical experiments based on a URANS approach was performed. Previous investigation [9] has shown the suitability of unsteady URANS rather than steady RANS to model the large-scale macroscopic flow pulsations which often occur in tight space rod bundles, as revealed by several experiments [8]. For the turbulence model, the inherent anisotropy of the Reynolds stresses in the gap region between the fuel rods and the presence of secondary flows demands the use of robust turbulence models, e.g. like the  $k-\omega$  SST but preferably an anisotropic nonlinear model like the  $k-\epsilon$  Shih model [8,9].

Based on the surface area of the inlet, the imposed experimental mass flow rate,  $\dot{m}_e$ , leads to an average inlet velocity of  $\bar{U} = 10.3 \text{ m/s}$ . Here, periodic boundary conditions are applied at the outlet of the numerical domain for all velocity components and the pressure. On the sloped lateral surfaces, symmetry

boundaries are imposed, while on the surface of the rods non-slip conditions are applied. For further clarification, in Figure 2 the numerical domain with the imposed boundary conditions is shown.

As already mentioned, in the numerical analysis of Hooper's sub-channel the working fluid is air, however in this paper different types of fluids, namely water and liquid lead, are also investigated to understand the sub-channel flow dynamics. The latter is especially relevant in the design of LMFRs since it is used as the primary coolant source. For such cases, changes in the sub-channel geometry are applied in comparison with Hooper's configuration, e.g., a triangular pitched pattern and a domain with different axial extension. In this geometry, the pitch-to-diameter ratio is  $P/D=1.32$ , which value is much larger than the corresponding ratio of Hooper's sub-channel and representative of a fuel assembly configuration using liquid lead as a coolant.

As the  $P/D$  ratio increases, a different flow dynamics in comparison with a lower  $P/D$  sub-channel geometry tends to develop, particularly, the macroscopic flow pulsations observed in hydraulic experiments decrease in intensity [8]. In this paper, such dynamics for different types of coolant fluids has been assessed in the sub-channel geometry shown in Figure 3. This geometry consists of a triangular pitched sub-channel configuration which is typical of LMFRs fuel bundles. For the simulations performed with this numerical domain, a similar set of boundary conditions as used in Hoopers sub-channel simulations is used.

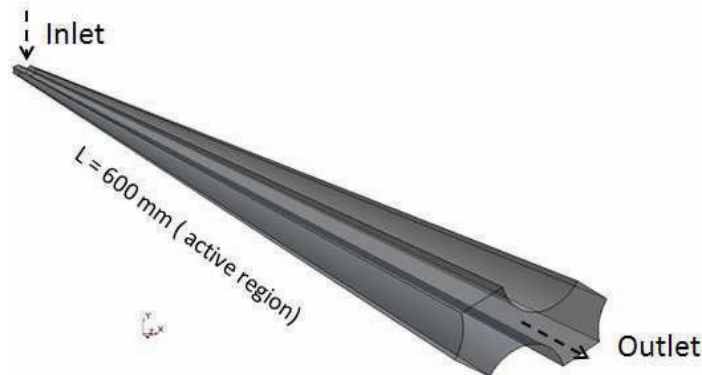


**Figure 3. Numerical domain of a triangular pitched pattern of a sub-channel geometry with  $P/D=1.32$ . The inlet and outlet region is shown. The dashed arrows indicate the main direction of the flow. On the sloped lateral sides symmetric boundaries are applied.**

For the triangular pitched pattern sub-channel, the inlet mass flow rate of liquid lead is set to  $\dot{m}_e = 1.536 \text{ kg/s}$ , which leads to an averaged velocity of  $\bar{U} = 1.21 \text{ m/s}$  at the inlet. In this case, fluid properties of liquid lead at a temperature of 675 K were used [11]. Under such thermal conditions, the Prandtl number for liquid lead is  $Pr = 0.02$ . Based on the hydraulic diameter of the sub-channel of Figure 3, the bulk Reynolds number of the experiments is  $Re_{bulk} = 46145$ .

In addition, the coolant flow in Hooper's sub-channel geometry is considered, where the sub-channel flow and the estimation for a feasible DNS resolution of Hooper's case will be discussed. Subsequently, analyses are performed on what are the consequences for the sub-channel flow dynamics as the coolant fluid is changed in the sub-channel geometry typical of a LMFR.

### 3. HOOPER'S SUB-CHANNEL CONFIGURATION

In this section, the results of the sub-channel flow of Hooper's bare rod bundle configuration are discussed. Initially, the focus is on the dynamics and large-scale macroscopic behavior of the flow at identical mass flow rate of the experiments, i.e.,  $\dot{m}_e = 0.052 \text{ kg/s}$ . These results will form our reference case after which the results of the scaled mass flow rate are discussed and compared. For a qualitative impression of the development of the flow within the sub-channel geometry of Hooper's configuration, Figure 4 shows the results of the velocity magnitude for this case.

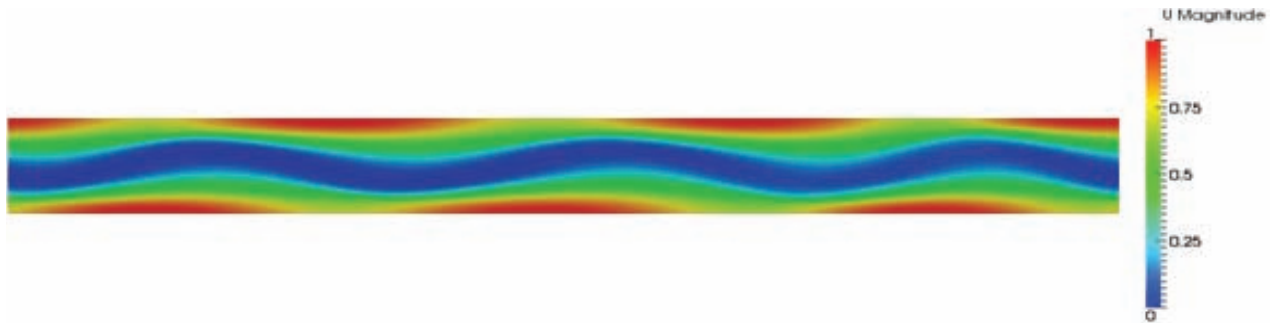


**Figure 4.** URANS ( $k-\omega$  SST model) results for the velocity magnitude for Hooper's sub-channel at identical mass flow rate of the experiments. Contours are shown for the plane- $xz$  at  $y=0$ . Flow direction is from left to right. The working fluid is air. The bulk Reynolds number (based on the hydraulic diameter) is approximately 49000.

Clearly, the macroscopic flow processes, i.e., large-scale macroscopic oscillations, which enhance eddy diffusion in sub-channel configurations of bare rod bundles are well captured with URANS. These pulsations strongly correlate with the periodic flow pulsations experimentally observed in Hooper's experiments [6,8].

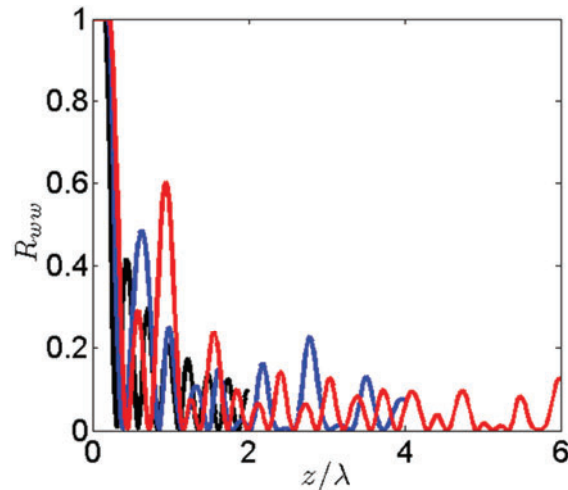


**Figure 5.** URANS results of the centerline streamwise two point autocorrelation function for several domains lengths. For all cases, the experimental air flow rate is, i.e.,  $\dot{m} = 0.052 \text{ kg/s}$ . Results are shown for an axial domain length of  $2\lambda$  (black line),  $4\lambda$  (blue line) and  $6\lambda$  (red line).

In these URANS simulations, the axial length of the numerical domain encompasses approximately  $4\lambda$ , where  $\lambda=0.318$  m is the averaged wave-length associated with one period of oscillation. To verify the sensitivity of the flow dynamics to the selected domain length, the axial length of the numerical domain within the range  $2\lambda \leq 4\lambda \leq 6\lambda$  has been varied. As already mentioned, here periodic conditions in the streamwise z-direction were used, since it is assumed that flow statistics are homogenous, i.e., independent, along this coordinate. To verify whether this assumption is realistic for the sub-channel flow under consideration, the behavior decay of the two point spatial autocorrelation function was investigated for numerical domains of different axial lengths. In Figure 5 the results of the spatial autocorrelation are shown, where for all cases the same mass flow rate of Hooper's experiments was used.

As can be seen, for the domain with axial length  $6\lambda$  a sufficient decay of the two point streamwise correlation, i.e.  $R_{ww} \approx 0.1$ , is fully established, while the domain with axial length of  $2\lambda$  is clearly not enough for the realistic use of periodicity. Since a careful selection of the domain extension is highly desirable for the high fidelity DNS to be performed, the numerical domain with axial length of  $4\lambda$  has been selected. The results show that the fall-off of the two-point autocorrelation function is already reasonable, albeit not completely sufficient to eliminate all effects of the streamwise periodic boundary conditions. Next, the relevant turbulent scales, e.g. Kolmogorov scales,  $\eta$ , and Taylor micro-scales,  $\lambda_g$ , have been estimated for the reference case with the selected length of  $4\lambda$ . For both scales, this estimation was carried out assuming homogenous isotropic turbulence [12]. Results for the typical turbulent scales are shown in Figure 6 for the reference case.

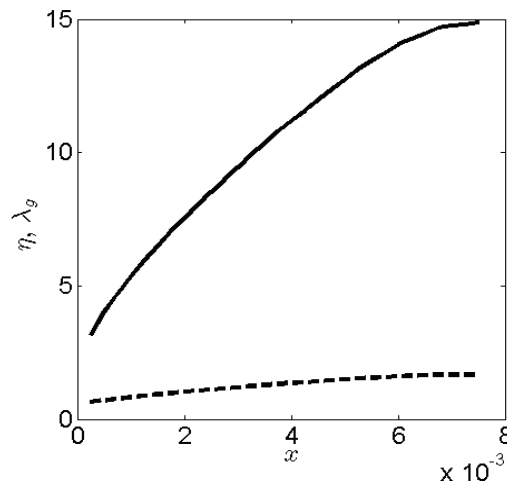


**Figure 6. Estimation results of Kolmogorov scales,  $\eta$  (dashed line) and Taylor micro-scales,  $\lambda_g$  (solid line), along the spanwise x-direction. Both flow scales are normalized by the ratio between the air kinematic viscosity and the average friction velocity  $u^*$ . Results are shown for the case with the experimental air flow rate, i.e.,  $\dot{m} = 0.052$  kg/s which correspond to the friction Reynolds numbers of  $Re_\tau = 2200$ .**

Considering the original air flow rate of the experiments, a simple estimation, based on the characteristic turbulent scales of Hooper's sub-channel, indicates that a volume mesh discretized with approximately 23 billion points would be required to resolve the spectrum range of turbulent scales up to the dissipation range for a numerical domain of axial length of  $4\lambda$ . In fact, from the computational point of view, such spatial discretization is far too expensive. To reduce the required resolution, in this paper we calibrate the original mass flow rate,  $\dot{m}_e = 0.052$  kg/s. Based on this approach, a successive reduction of  $\dot{m}_e$ , which corresponds to a friction Reynolds number of  $Re_\tau = 2200$ , up to  $\dot{m} = 0.0065$  kg/s, i.e.,  $Re_\tau = 275$ , is performed.

Despite the subsequent reduction of the original air flow rate, the macroscopic behavior of the characteristic axial oscillations of the flow is retained. As an example, Figure 7 shows the contours of the velocity magnitude for several cases with the calibrated flow rates.

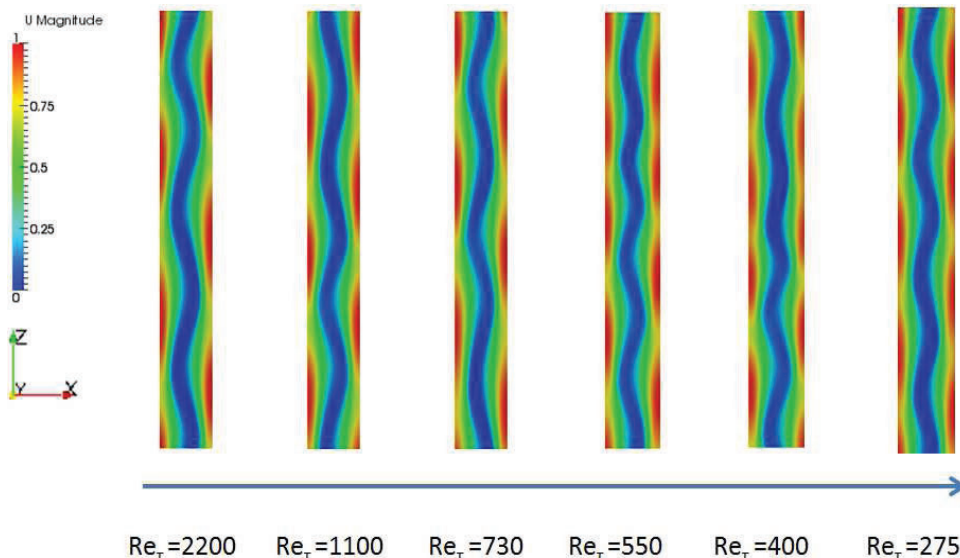


Figure 7. URANS ( $k-\omega$  SST model) results of the velocity magnitude of Hooper's sub-channel for mass flow rates varying within the range  $0.0065 \text{ kg/s} \leq \dot{m} \leq 0.052 \text{ kg/s}$ , which corresponds to the friction Reynolds number range of  $275 \leq Re_\tau \leq 2200$ . The coolant flow is air. Contours are shown for the plane-xz at  $y=0$ .

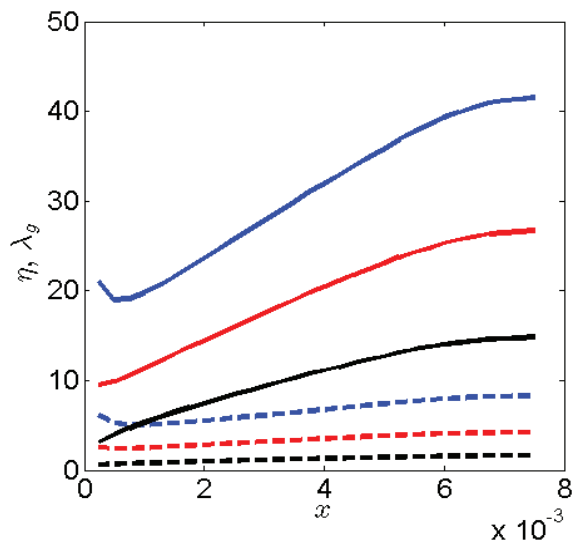
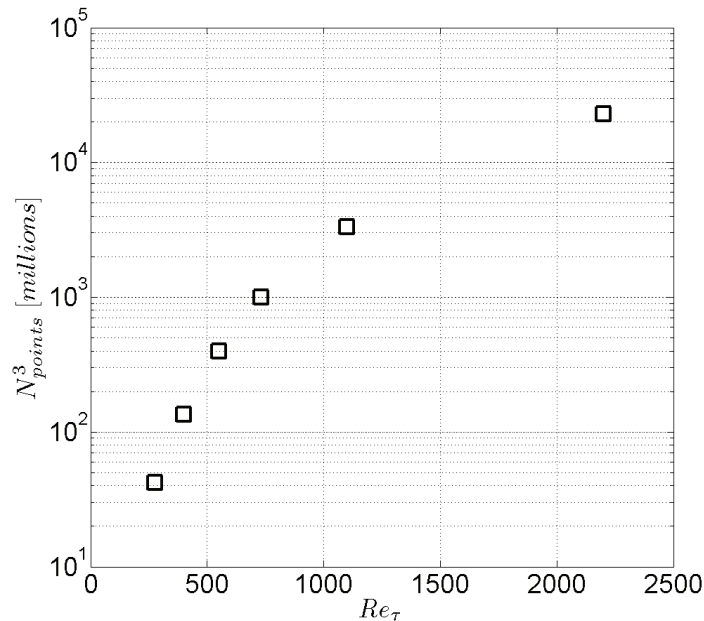


Figure 8. Estimation results of normalized Kolmogorov scales,  $\eta$  (dashed line) and Taylor micro-scales,  $\lambda_g$ , (solid line) along the spanwise x-direction for several inlet mass flow rates. Results are shown for the cases with air flow rates of  $\dot{m} = 0.0065 \text{ kg/s}$  (blue lines),  $\dot{m} = 0.013 \text{ kg/s}$  (red lines) and  $\dot{m} = 0.052 \text{ kg/s}$  (black lines), which correspond to the following friction Reynolds numbers  $Re_\tau = 275$ ,  $Re_\tau = 550$  and  $Re_\tau = 2200$ , respectively.

As can be observed, despite the systematic reduction of the original mass flow rate by a factor of eight, the flow dynamics remains roughly identical in all cases. Major differences are only due to the frequency of the large-scale oscillation which tends to increase as the air flow decreases. Adopting a similar procedure to estimate the flow scales  $\eta$  and  $\lambda_g$ , Figure 8 shows the effects of the subsequent reduction of the mass flow rate on the estimated size of the referred turbulent scales.

Through the rescaling of the original air flow rate the required resolution for a detailed DNS also decreases. Results in Figure 9 show the subsequent reduction of the required spatial resolution in terms of the friction Reynolds number associated with the calibrated flow rates.



**Figure 9.** Estimation results of the total number of grid points required for a fully detailed reference DNS of Hooper’s sub-channel flow. Results are shown as a function of the friction Reynolds numbers  $Re_\tau$  within the range  $275 \leq Re_\tau \leq 2200$ , which corresponds to air flow rates of  $0.0065 \text{ kg/s} \leq \dot{m} \leq 0.052 \text{ kg/s}$ .

As can be seen, through the calibration procedure of the original mass flow rate, the rescaled air flow rate of  $\dot{m} = 0.0094 \text{ kg/s}$ , i.e.,  $Re_\tau = 400$ , requires a volume mesh of roughly 135 million grid points to resolve the flow scales up to the dissipation range. In fact, this level of resolution is computationally affordable for the accomplishment of a reference DNS of the analyzed sub-channel. Since the lower rate case, i.e.,  $Re_\tau = 275$ , could lead to flow relaminarization, the mass flow rate of  $\dot{m} = 0.0094 \text{ kg/s}$  has been selected for targeted DNS computations. It is worth mentioning that, the aforementioned mesh estimation is performed on a selected RANS computational domain, which is not sufficient enough to replicate the real Hooper case for a high fidelity DNS computation. Therefore, the target DNS shall be performed on the original Hooper case domain, which is four times the size of previously considered RANS domain. This will eventually increase the overall mesh from 135 to 540 million grid points.

#### 4. LMFR'S SUB-CHANNEL CONFIGURATION

In this section, flow analyses of a sub-channel geometry with a P/D ratio larger than the corresponding ratio of Hooper's configuration are performed. In addition, also the configuration of the rods changes from a rectangular pitch to a triangular pitch.

In order to establish the accuracy of these simulations, initially the sensitivity of the flow field has been verified, corresponding to a liquid lead sub-channel flow, to the spatial grid resolution. Results in Figure 10 show that grid independence is already sufficiently achieved for the grid discretized with approximately 1.4 million points. Based on these results, in the sequence this grid resolution has been restricted as reference mesh to assess the sub-channel flow dynamics of different working fluids.

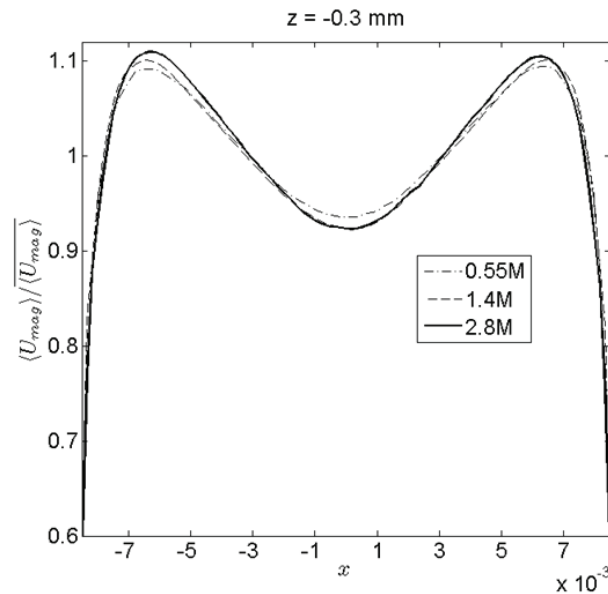


**Figure 10. Time-average cross section profiles of the normalized mean velocity magnitude for different grid resolutions. Profiles are extracted at  $z = -0.3$  mm, which corresponds to a streamwise location on half of domain. The mean velocity is normalized by the mean velocity magnitude spatially averaged along the x-direction. The working fluid in all cases is liquid lead. The bulk Reynolds number (based on the hydraulic diameter) is  $Re_{bulk} = 46145$ .**

As a first step, the working fluid is varied from liquid lead to air. Despite the large variability of the physical properties, e.g., density and dynamics viscosity, of both fluids, the bulk Reynolds number,  $Re_{bulk} = 46145$ , has been retained for all cases. Results in Figure 11 show that although the velocity magnitude for air varies within a factor of approximately 100 when compared with the results for liquid lead, the flow topology is identical for both cases.

A quantitative comparison between both fluids is shown in Figure 12. As can be observed, the flow physics is identical up to first order statistical quantities, e.g., mean velocity magnitude, for air and liquid lead since the mean profiles are fully symmetric with respect to  $x = 0$  for all cases. In this paper, only results for liquid lead and air are shown, since identical results are obtained in case of water. In fact, the water sub-channel flow also exhibits identical profiles up to second order statistics when compared with the liquid lead case. These set of results clearly show that despite the use of different working fluids, the sub-channel flow dynamics is identical in all cases as long as the Reynolds number remains the same.

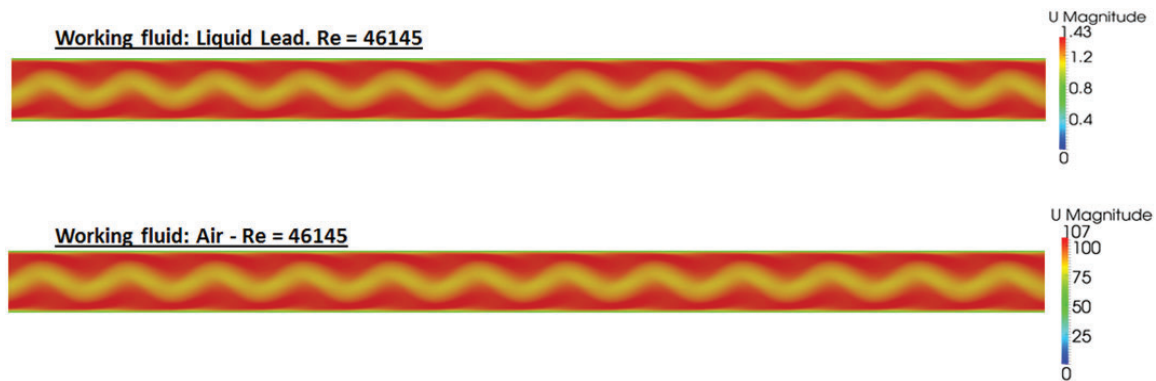


Figure 11. Flow snapshot of the instantaneous velocity magnitude for liquid lead (top) and air (bottom) on a  $xz$ -plane extracted at  $y=0$ . For both cases, results were obtained using URANS with  $k-\epsilon$  Shih model.

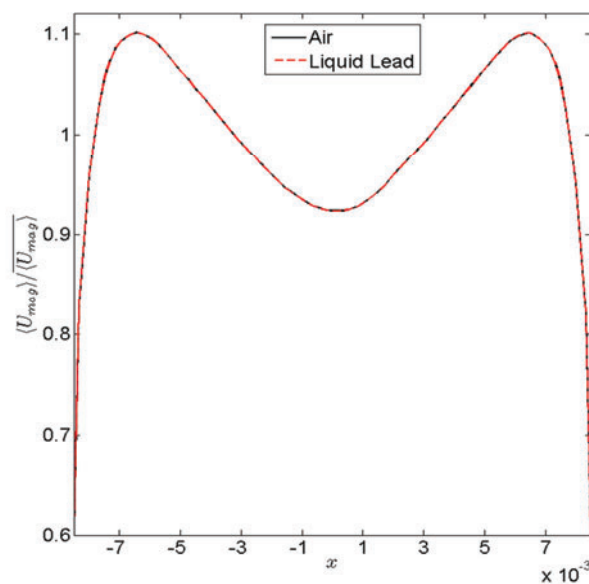


Figure 12. Time-average cross section profile of the normalized mean velocity magnitude for liquid lead and air. Profiles are extracted at  $z=300$  mm, which corresponds to a streamwise location on half of domain. Both quantities are normalized by the corresponding quantity spatially averaged along the  $x$ -direction.

The occurrence of large-scale flow pulsations can be critical in case one needs to assess flow induced vibrations in lattice rod bundles. While the existence of these wavy patterns further enhances momentum and heat transport mixing in the gap regions between the fuel rods, it often leads to similar spatially periodic oscillations in the wall shear stress magnitude,  $\tau_w$ . The latter effect is not desirable since an oscillating wall shear stress can cause substantial mechanical loads on the fuel rod's surface [9]. Figure 13 shows the contours of the wall shear stress magnitude,  $\tau_w$ , for the top rod's surface of a sub-channel flow with liquid lead and air.

As can be seen, the large-scale flow pulsation has a significant effect on  $\tau_w$  such that it follows the general oscillatory behavior of the main flow. As expected, the wall shear stresses on the rod's surfaces increase as the mean flow velocity gets high. To provide a quantitative analysis of the variability of  $\tau_w$  for both fluids, a normalized amplitude variation,  $\sigma_A$ , based on the maximum and minimum values of  $\tau_w$ , is

defined along the rod's wall. These results are shown in Figure 14 for all working fluids assessed, i.e., liquid lead, water and air.

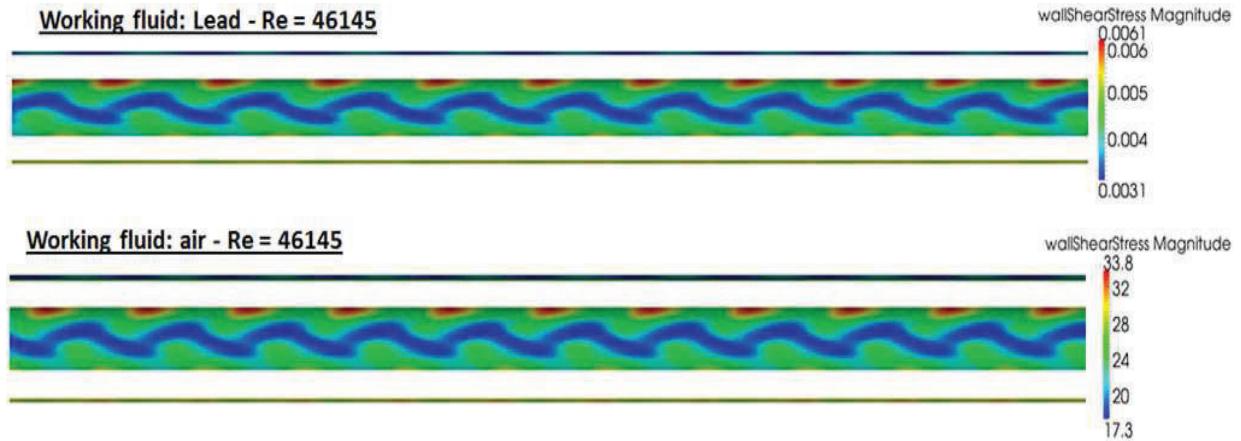


Figure 13. Flow snapshot of the instantaneous wall shear stress magnitude for liquid lead (top) and air (bottom) on a  $xz$ -plane extracted at  $y=0$ . For both cases, results were obtained using URANS with the  $k-\varepsilon$  Shih model.

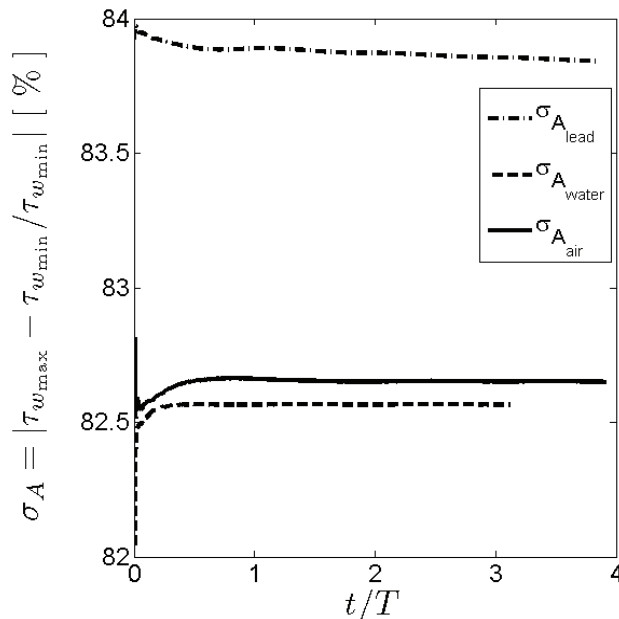


Figure 14. Largest amplitude variation,  $\sigma_A$ , of the normalized cumulative wall shear stress magnitude  $\tau_w$  as a function of time for three different working fluids: liquid lead, water and air. The time  $t$  is normalized by the time  $T$ , where  $T = L_z/\bar{U}$  corresponds to the time spent for the main flow to go through the domain along the streamwise direction.

Clearly, a large variability of the amplitude of the wall shear stress magnitude, i.e.,  $\sigma_A > 80\%$ , is observed for all cases. In addition, the variation of  $\sigma_A$  is almost identical for all working fluids such that a maximum difference of less than 1.4% is observed when the amplitude variation  $\sigma_A$  of the liquid lead flow, for instance, is directly compared to the water sub-channel flow. This is due to the fact that the bulk

Reynolds number is retained in all cases, such that the amplitude variation of the wall shear stress pulsation is roughly the same for all coolant fluids.

## 5. CONCLUSIONS

In this paper, a set of URANS simulations of sub-channel flows commonly found in bare fuel rod bundles were performed. Currently, the lack of a reference detailed data in such sub-channel geometries often limits the detailed knowledge of local flow effects, such as mixing and heat transfer transport within the reactor fuel assemblies. This situation is especially severe for design and safety analysis of new promising nuclear reactor technologies such as the case of liquid lead cooled fast reactors. To fill this knowledge gap, in this paper an approach is developed to obtain a feasible computation domain of a bare rod bundle sub-channel configuration in which a thorough knowledge of local flow phenomena can be further pursued.

Initially, a squared pitched tight lattice sub-channel geometry of  $P/D=1.107$  was investigated, which corresponds to the flow configuration of Hooper's hydraulic experiments. Using the same air mass flow rate of the experiments, the macroscopic flow pulsation was successfully reproduced. Based on these results an estimation of the required resolution for a reference simulation of a sub-channel geometry led to a spatial grid resolution which is far too computationally expensive to be performed, in case the same mass flow rate of the experiments is maintained. To overcome this difficulty, a systematic calibration of the reference mass flow rate has led to a feasible spatial resolution, e.g., volume mesh discretized with roughly 135 million points for  $Re_\tau = 400$ , for a reference simulation of the sub-channel flow under investigation.

In addition, the flow dynamics within a sub-channel configuration typical of LMFR rod bundles, was also considered, where numerical computations were performed for a triangular pitched lattice sub-channel geometry of  $P/D=1.32$ . In these simulations, the sub-channel flow was varied by considering several types of working fluids, e.g., air, water and liquid lead. The results show that the general aspects of the flow, i.e., topology (macroscopic flow oscillations) and the flow field dynamics (velocity field and wall shear stress magnitude), remain the same for sub-channel flows of fluids with different Prandtl numbers as long as the bulk Reynolds number is kept the same in all cases.

Combined, these results consistently show that the reference simulation data to be obtained for a sub-channel flow where the working fluid is air, for instance, will also serve as a validation tool for other CFD modeling approaches of liquid lead flows in bare rod sub-channels of LMFRs.

## ACKNOWLEDGMENTS

The work described in this paper is funded by the Dutch Ministry of Economic Affairs. The Hooper case simulations, presented in this paper, were performed at Swierk Computing Centre in a framework of the the EU and MSHE grant no. POIG.02.03.00-00-013/09.”

## REFERENCES

1. IAEA, 2012. Status of Fast Reactor Research and Technology Development. Technical Report 474, ISBN 978-92-0-130610-4, Vienna, Austria.

2. T. Krauss, L. Meyer, “Experimental investigation of turbulent transport of momentum and energy in a heated rod bundle”, *Nuclear Engineering & Design*, **180**, pp. 185-206 (1998)
3. Roelofs, F. et al., “Review of fuel assembly and pool thermal hydraulics for fast reactors”, *Nuclear Engineering & Design*, **265**, 1205-1222 (2013)
4. IAEA, 2013. Status of Innovative Fast Reactor Designs and Concepts. A Supplement to the IAEA Advanced Reactors Information System (ARIS). IAEA Booklet 13.42471, Vienna, Austria.
5. M. Frogheri, A. Alemberti, L. Mansani, The Lead Fast Reactor: Demonstrator (ALFRED) and ELFR Design. FR13, Paris, France (2013).
6. J.D. Hooper, “Developed single-phase turbulent flow through a square-pitch rod cluster”, *Nuclear Engineering & Design*, **45**, pp. 311-323 (1980)
7. K.D. Hamman, A.R. Berry. “A CFD simulation process for fast reactor fuel assemblies”, *Nuclear Engineering & Design*, **240**, pp. 2304-2312 (2010)
8. L. Meyer, “From discovery to recognition of periodic large scale vortices in rod bundles as source of natural mixing between sub-channels - a review”, *Nuclear Engineering & Design*, **240**, pp. 1575-1588 (2010)
9. L. Chandra, F. Roelofs, E.M. Komen, E. Baglietto, “Unsteady RANS and LES Analyses of Hooper’s Hydraulics Experiment in a Tight Lattice Bare Rod-bundle”, *NUTHOS-8, N8P0218*, Shanghai, China (2010)
10. OpenFOAM project web page. <http://www.openfoam.org> 2014 .
11. Nuclear Energy Agency, *Handbook on Lead-bismuth Eutectic Alloy and Lead Properties, Materials Compatibility, Thermal-hydraulics and Technologies* (2007)
12. S.B. Pope, *Turbulent Flows*, Cambridge University Press (2006)